EARTHQUAKE ENGINEERING AND STRUCTURAL DYNAMICS
Earthquake Engng Struct. Dyn. 2000; **29**: 399–418

Parameters determination for a linearly inhomogeneous half-space using characteristics of the time-harmonic surface waves

Grigori Muravskii*

Geotechnical Department, Faculty of Civil Engineering, Technion, 32000 Haifa, Israel

SUMMARY

The paper presents a study of time-harmonic surface waves in a linearly inhomogeneous half-space. The study is based on the solution of that problem for an arbitrary (from 0 to 1/2) value of Poisson's ratio. Vertical vibrations due to a vertical harmonic force, which at large distances from the force represent Rayleigh-type waves, and transverse horizontal vibrations due to a horizontal force, which at large distances form waves of Love's type, are considered in detail. Material damping is taken into consideration. Inhomogeneity significantly affects relationships connecting wave characteristics and the frequency of vibration, and it is shown in the paper how this fact can be used for determining material properties (surface shear modulus, degree of inhomogeneity, damping ratio) with the help of experimental results concerning wave propagation over the surface of the half-space. It is shown that for forced waves the relationship between the wave phase angle and distance can significantly differ from a straight line, i.e. the wave number varies with distance. Therefore, it is desirable to relate experimental and theoretical results to such parts of wave propagation line, which correspond to same phase angle intervals. Copyright © 2000 John Wiley & Sons, Ltd.

KEY WORDS: time-harmonic vibration; inhomogeneous half-space; material damping; Rayleigh-type waves; Love-type waves; wave dispersion

INTRODUCTION

Solutions concerning time-harmonic problems for a continuously inhomogeneous half-space subjected to forces applied to the surface of the half-space are related mostly to plane and axisymmetric cases [1–8]. Recently papers have been published by the author dealing, in the context of a three-dimensional problem, with vertical and horizontal forces applied to an incompressible inhomogeneous half-space with the linearly varying shear modulus [9], a half-space with the exponentially varying modulus increasing to infinity with depth [10], and an

* Correspondence to: Grigori Muravskii, Geotechnical Department, Faculty of Civil Engineering, Technion, 32000 Haifa, Israel.

Received 3 July 1997
Revised 18 March 1999
Accepted 14 September 1999

inhomogeneous half-space with shear modulus varying as a polynomial of exponential functions and bounded at infinite depth [11]. In Reference [12], time-harmonic Green functions for an isotropic elastic linearly non-homogeneous half-space are constructed for arbitrary values of Poisson ratio from 0 to 1/2, unlike papers [1, 2, 8, 9, 13] which deal only with an incompressible half-spaces. Note that free vibrations of a compressible linearly inhomogeneous half-space were studied in Reference [14] where approximate analytic solutions in combination with numerical methods were used. The main goal of the present paper is the study of characteristics of forced time-harmonic surface waves in a linearly inhomogeneous half-space and applications of the results to soil properties determination using experimental data, provided the actual variation of the soil shear modulus with depth can be approximated with the assumed linear law (see Reference [15]). Wave dispersion (the dependence of wave velocities on frequencies or wave lengths) associated with inhomogeneity is discussed in Reference [16], where experimental results are used for estimating soil stiffness changing with depth. In References [17, 18], dispersive properties of surface waves were studied using theoretical and experimental approaches. Contrary to works [16–18], dealing with the steady-state vibration technique, the method utilizing spectral analysis of surface waves (SASW) [19–23], is widely used for determination of soil foundation properties through surface wave characteristics. Actually, both methods use the variation (caused by inhomogeneity) of the Rayleigh wave velocity (V_R) with frequency (or with wavelength). When employing the methods, the main problem consists in reconstructing the profile from a dispersion curve or from other information concerning wave characteristics at different frequencies. As a first step one uses the simplest way of obtaining the shear wave velocity profile by application of the dispersion curve: assumes that the depth of sampling (equivalent depth) is from 0.33 to 0.5 of the wavelength [16, 19]. The estimation of the equivalent depth has been done by Gazetas [24] for soil deposits with wave velocities increasing from surface to baserock according to several laws and Vrettos [17] for a half-spaces with exponentially varying shear modulus from a value at the surface of the half-space to a limit value at infinite depth. In papers dealing with SASW, a trial and error process is applied on the Haskell–Thomson's [25,26] matrix for multilayered media or other solutions in this area [27,28]. According to this process, the considered soil is assumed as a system of layers having constant characteristics, which should be chosen to obtain an acceptable proximity between theoretical and experimental dispersion curves. It should be noted that in the case of inhomogeneous half-spaces, a definite unique dispersion curve corresponding to forced vibrations does not exists. In the subsequent text will be shown that phase lines presenting the relationships between the phase of complex amplitudes of vibration and point distances from the acting force can deviate significantly from a straight line, i.e. wave characteristics at dissimilar parts of the line of wave propagation can noticeably differ from each other. Similar results can be found also in Reference [6]. Analogously, in Reference [22] for some examples of a layered half-space, is shown that the location of receivers used in SASW can influence significantly the obtained dispersion curves, especially at low frequencies. Up to now, determination of soil characteristics using dispersive properties of time-harmonic surface waves in inhomogeneous elastic bases has been performed with consideration of vertical vibrations due to vertical forces (Rayleigh waves). In this paper, much attention is given to analysis of the waves which are closely related to waves of Love's type. In the paper, a comprehensive analysis of the influence of material damping on characteristics of forced surface Love' and Rayleigh's waves is made. The obtained results allow to determine the damping ratio of soil with the help of corresponding experimental data. In this brief survey, we leave without of consideration a great number of analytical-numerical and numerical works on wave propagation

in layered media with constant material properties in every layer. A bibliography on this subject and also the application of a method of a system of thin homogeneous layers for an approximation of a soil can be found in Reference [27].

GENERAL SOLUTION

We use the cylindrical coordinates r, ϑ, z with z-axis directed towards the half-space whose surface corresponds to $z = z_0 > 0$. The half-space is characterized by constant Poisson's ratio v and density ρ, and shears modulus $G = G(z)$ which depends on the z-coordinate. According to References [12–16], amplitudes of vibrations u_r, u_ϑ, u_z in the directions of the co-ordinate lines, corresponding to a vertical harmonic force $P_0 \exp(\mathrm{i}\omega t)$ (ω is the circular frequency and t is time) uniformly distributed over a circular area of radius R on the surface of an elastic isotropic inhomogeneous half-space, can be represented in the form

$$u_r = -\frac{P_0}{\pi}\int_0^\infty \frac{J_1(kR)}{R} J_1(kr)\frac{c_{22}q_1(z,k) - c_{21}q_2(z,k)}{D}\,\mathrm{d}k \tag{1a}$$

$$u_z = -\frac{P_0}{\pi}\int_0^\infty \frac{J_1(kR)}{R} J_0(kr)\frac{c_{22}w_1(z,k) - c_{21}w_2(z,k)}{D}\,\mathrm{d}k \tag{1b}$$

$$u_\vartheta = 0 \tag{1c}$$

where

$$D = c_{11}c_{22} - c_{12}c_{21} \tag{2a}$$

$$c_{1j} = \bar{e}_j(z_0) - 2kG(z_0)q_j(z_0) \tag{2b}$$

$$c_{2j} = \bar{\chi}_j(z_0) - 2kG(z_0)w_j(z_0) \quad (j = 1, 2) \tag{2c}$$

In above equations, J_0 and J_1 denotes Bessel's functions; $\bar{\chi}_1, \bar{e}_1, q_1, w_1$ and $\bar{\chi}_2, \bar{e}_2, q_2, w_2$ are two solutions (satisfying the condition of absence of sources when $z \to \infty$) of the system of equations, given in Reference [8, 9, 12].

In the case of a horizontal force $Q_0 \exp(\mathrm{i}\omega t)$ uniformly distributed over a circle of radius R on the surface of the half-space, amplitudes have the form [8–12]

$$u_r = \hat{u}_r \cos\vartheta \tag{3a}$$

$$u_\vartheta = \hat{u}_\vartheta \sin\vartheta \tag{3b}$$

$$u_z = \hat{u}_z \cos\vartheta \tag{3c}$$

$$\hat{u}_r = \frac{Q_0}{\pi}\int_0^\infty \frac{J_1(kR)}{R}\left[[q(z,k) - p(z,k)]\frac{J_1(kr)}{kr} - q(z,k)\,J_0(kr)\right]\mathrm{d}k \tag{4}$$

$$\hat{u}_\vartheta = \frac{Q_0}{\pi}\int_0^\infty \frac{J_1(kR)}{R}\left[[q(z,k) - p(z,k)]\frac{J_1(kr)}{kr} + p(z,k)\,J_0(kr)\right]\mathrm{d}k \tag{5}$$

$$\hat{u}_z = \frac{Q_0}{\pi}\int_0^\infty \frac{J_1(kR)}{R} w(z,k)\,J_1(kr)\,\mathrm{d}k \tag{6}$$

where

$$q(z,k) = \frac{c_{11}q_2(z,k) - c_{12}q_1(z,k)}{D} \tag{7}$$

$$w(z,k) = \frac{c_{11}w_2(z,k) - c_{12}w_1(z,k)}{D} \tag{8}$$

$$p(z,k) = p_1(z,k) \Big/ \left[G(z_0) \frac{\mathrm{d}p_1(z_0 k)}{\mathrm{d}z} \right] \tag{9}$$

The additional function $p_1(z,k)$ is a solution (satisfying the radiation condition at infinity) of the equation

$$G\frac{\mathrm{d}^2 p_1}{\mathrm{d}z^2} + \frac{\mathrm{d}G}{\mathrm{d}z}\frac{\mathrm{d}p_1}{\mathrm{d}z} + (\rho\omega^2 - k^2 G)p_1 = 0 \tag{10}$$

Waves of Rayleigh's type are connected with zeros of the demoninator D in expressions (1a), (1b), (7), (8). Love-type waves correspond to the poles of the function $p(z,k)$ entering equations (4) and (5). Calculations in References [9, 11, 12] show that poles of the function $p(z,k)$ lead to an increase (compared to the static case) of displacements with distance from the acting force only for the components u_ϑ. According to equations (3b), these components represents for $\vartheta = \pi/2$ amplitudes of vibrations (in the direction of the acting force) in the plane that passes through the point of force application perpendicularly to the force direction. One can see in this situation a similarity to the so-called anti-plane problem in which only shear deformations are inherent; it can be shown that the anti-plane solution is expressed with the help of the function $p(z,k)$.

CASE A: A HORIZONTAL FORCE

We will consider transverse horizontal surface waves represented by the amplitudes $\hat{u}_\vartheta$ in a linearly inhomogeneously half-space. Characteristics of these waves can be effectively used for determination of half-space properties.

In Reference [12], two fundamental solutions $q_j(z,k)$, $w_j(z,k)$, $\bar{e}_j(z,k)$, $\bar{\chi}_j((z,k)$ $(j = 1, 2)$ and the solution $p_1(z,k)$ have been obtained for the following variation of the shear modulus with the depth co-ordinate z:

$$G(z) = mz \tag{11}$$

where m is a positive constant. The constant m can be written in the form $m = G(z_0)/z_0$, where z_0 corresponds to the z-value at the surface. In order to introduce dissipative properties of the material into the solution one can consider the shear modulus as a complex quantity

$$G(z_0) = G_0(1 + \mathrm{i}\varepsilon) \tag{12a}$$

$$m = m_0(1 + \mathrm{i}\varepsilon) \tag{12b}$$

$$m_0 = G_0/z_0 \tag{12c}$$

where ε is a small positive value (ε is twice the damping ratio) and G_0 is the shear modulus at the surface for the non-dissipative case. Poisson's ratio is assumed to be real.

We will study further the amplitudes $\hat{u}_\vartheta$ generated by a point horizontal force at the surface of the half-space with the help of the following representation:

$$\hat{u}_\vartheta = -\frac{Q_0}{4\pi r G_0} S_\vartheta \tag{13}$$

where S_ϑ is the normalized amplitude which is related to the normalized amplitude S_{hh2} determined in Reference [12] as follows:

$$S_\vartheta = 2(1-\nu) S_{hh2} \tag{14}$$

The parameters influencing values of S_θ are ε, θ and a where

$$\theta = \omega z_0 (\rho/G_0)^{1/2} \tag{15a}$$

$$a = \omega r (\rho/G_0)^{1/2} \tag{15b}$$

We will represent results of calculations as functions of a for a number of fixed values of the parameter θ. Calculations show [and this is also seen from Equation (5)] that the amplitudes for sufficient large values of a are determined practically by the term $p(z,k)J_0(kr)$ in Equation (5), i.e. by the same function p which is associated with Love's waves in the case of anti-plane shear vibrations. The corresponding part of $\hat{u}_\vartheta$ can be called as the 'far-field solution'. For illustration, in Figure 1 the absolute values of normalized amplitudes S_ϑ are shown for $\varepsilon = 0$ and several values of θ according to the exact expression for S_ϑ and the above approximation (dashed lines). It can also be shown that phase angles of complex amplitudes of vibrations (from which one may determine propagation velocity) corresponding to the exact solution and the 'far-field solution' are all the more close to each other. Note that for $a \to 0$, the value of S_ϑ tends to $2(1-\nu)$ according to the static homogeneous solution; with increase of a, the influence on Poisson's ratio tends to diminish.

Consider the phase angle δ_ϑ of complex normalized amplitudes S_ϑ for several values of parameter θ and $\varepsilon = 0$, $\nu = 1/3$ (Figure 2). Corresponding curves, beginning with large enough values of a, are close to straight lines having the equation

$$\delta_\vartheta = b_\vartheta - k_\vartheta a \tag{16}$$

where b_ϑ is a constant that does not influence wave characteristics, and k_ϑ is the non-dimensional (related to the parameter a) wave number. The relation between k_ϑ and the dimensional wave number K_ϑ corresponding to distance r is determined from the following relationships:

$$k_\vartheta a = k_\vartheta \omega r (\rho/G_0)^{1/2} \tag{17a}$$

$$K_\vartheta = k_\vartheta \omega (\rho/G_0)^{1/2} \tag{17b}$$

For determining the relationship between k_ϑ and θ, we consider the intervals of variation of the parameter a where the phase angle δ_ϑ varies from -2π to -4π, from -4π to -6π, … , and

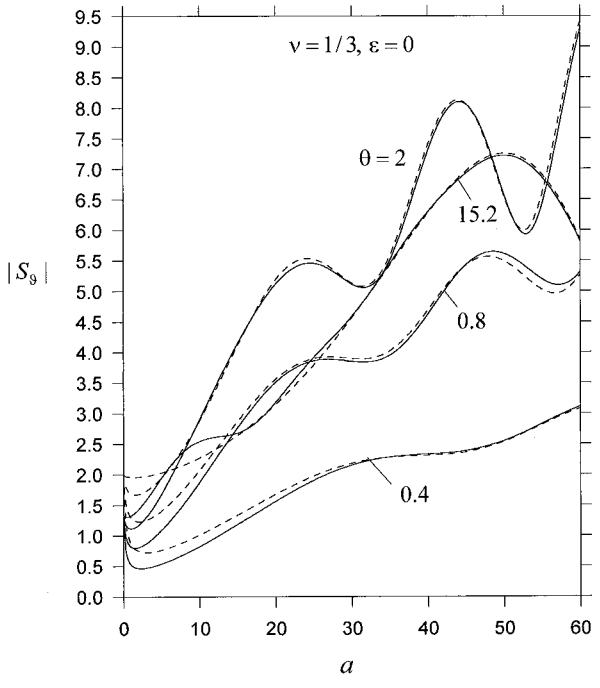

Figure 1. Absolute value of complex normalized horizontal amplitudes of vibrations; dashed lines are for far-field solution.

use the secant straight lines having these ordinates at the ends of the corresponding intervals of a. We will call these intervals 'second wave', 'third wave' etc. respectively. In Figure 2 corresponding intervals with non-dimensional lengths l_{II} and l_{III} are shown for 'second wave' and 'third wave', respectively (for $\theta = 2$). These terms are used for brevity; actually we do not deal with different waves but with definite parts of a complex wave (in sequel, inverted commas will be omitted). Actually, we use the term 'number of wave' introduced in Reference [16, pp. 111–114] where one can find corresponding explanations. Using the secant lines for a large number of values of parameter θ, we obtain the relationship shown in Figure 3 where the following variable λ is used as an argument:

$$\lambda = \frac{\theta}{0.9 + \theta} \tag{18}$$

This choice leads to proximity between the curves in Figure 3 and straight lines. Note that the value $\lambda = 1$ ($z_0 \to \infty$, $\theta \to \infty$) corresponds to the homogeneous half-space, for which k_ϑ should be equal to 1 for the pure shear waves. For the second wave, the calculated result for $\varepsilon = 0$ is 0.9676 instead of 1, and for subsequent waves it becomes closer to 1 (Figure 3). The discrepancy between curves for the second, third and fourth waves gives an estimation of deflection of phase

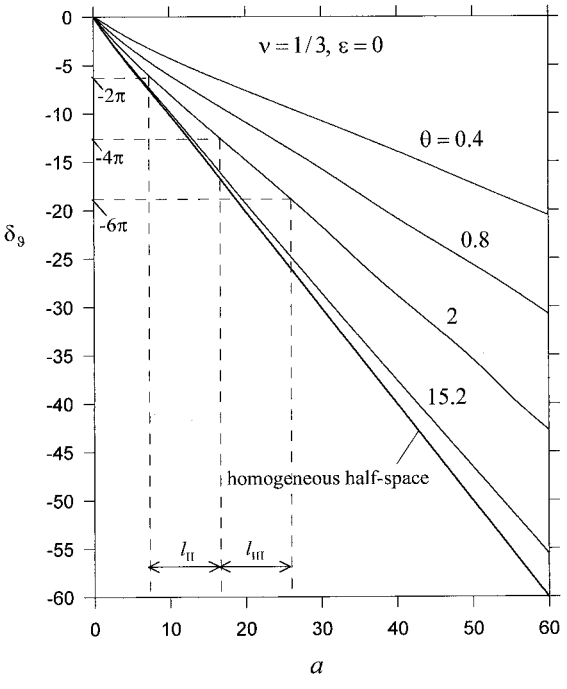

Figure 2. Phase angle of complex horizontal amplitudes of vibrations for some values of parameter θ.

lines shown in Figure 2, from straight lines. The following relation

$$k_\vartheta = \lambda = \frac{\theta}{0.9 + \theta} \tag{19}$$

is an approximation sufficient for practical applications when the second or third waves are used. Although the above results correspond to the case $\nu = 0.5$, they are also valid with sufficient accuracy for other values of Poisson ratio which influences amplitudes S_ϑ only at the interval of small values of parameter a (see Figure 1). This interval lies before the interval corresponding to the second wave.

Regarding the dissipative parameter ε [Figure 3(b)] leads to the conclusion that for the second and third waves, its influence on parameter k_ϑ is insignificant for values of ε not exceeding 0.2.

The obtained approximate relationship (19) between k_ϑ and θ can be used for an experimental determination of properties of soil foundation, provided that soil inhomogeneity can be approximated by the linear law. Consider a small footing on the surface of soil which oscillates in horizontal and possibly vertical directions. Note that the horizontal amplitudes (corresponding to the values $\hat{u}_\vartheta$) of points lying at the surface line, which passes through the centre of the footing perpendicularly to its horizontal component of vibration are not influenced by the vertical component of footing vibrations. Let ω_1 and $\omega_2 = \alpha\omega_1$ be two values of circular frequency.

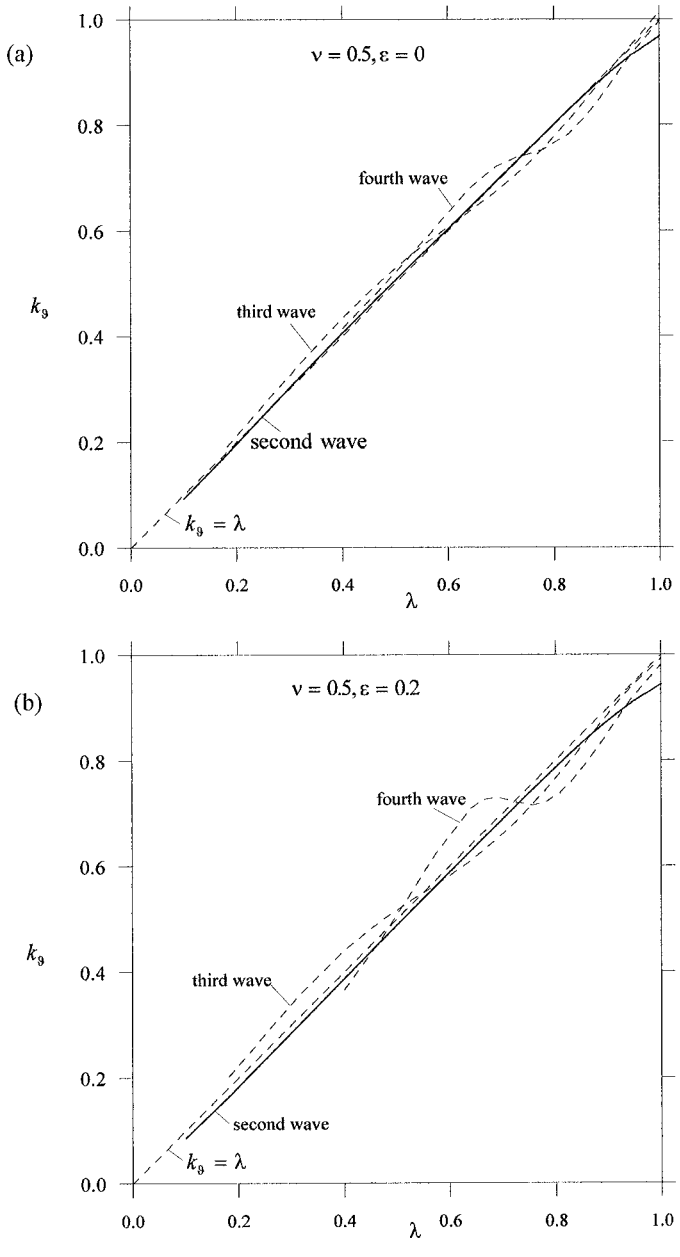

Figure 3. Non-dimensional wave number versus parameter $\lambda = \theta/(0.9 + \theta)$ for horizontal vibrations.

Suppose we know, from an experiment, the corresponding surface wavelengths for the second (third) wave, defined as the distance between the first (second) and second (third) points lying on the mentioned line and having the same phase of vibration as that of the horizontal motion of the footing. The corresponding non-dimensional wavelengths are shown in Figure 2. Such points can be found by moving of a receiver along the wave propagation line. The equation connecting the ratio of l_1 and l_2 and corresponding values of k_ϑ is as follows:

$$\frac{l_1}{l_2} = \frac{K_\vartheta(\theta_2)}{K_\vartheta(\theta_1)} = \frac{k_\vartheta(\theta_2)\omega_2}{k_\vartheta(\theta_1)\omega_1} \tag{20}$$

where θ_1 and $\theta_2 = \alpha\theta_1$ correspond to ω_1 and ω_2. Actually, Equation (20) is an equation for determining θ_1 provided the function $k_\vartheta = k_\vartheta(\theta)$ is known. Using Equation (19) we obtain

$$\theta_1 = \frac{0.9(\alpha - \beta)}{\alpha(\beta - 1)} \tag{21}$$

where

$$\beta = \frac{l_1\omega_1}{l_2\omega_2} = \frac{l_1}{\alpha l_2} \tag{22}$$

Further, knowing θ_1 and using Equation (15) specifying θ, we can obtain the parameter z_0 from the following relationships:

$$l_1 = \frac{2\pi}{K_\vartheta(\theta_1)} = \frac{2\pi}{k_\vartheta(\theta_1)\omega_1\sqrt{\rho/G_0}} = \frac{2\pi z_0}{k_\vartheta(\theta_1)\theta_1} \tag{23a}$$

$$z_0 = \frac{l_1\theta_1 k_\vartheta(\theta_1)}{2\pi} \tag{23b}$$

Knowing z_0 and ρ, the shear modulus G_0 can be found:

$$G_0 = \frac{z_0^2\omega_1^2\rho}{\theta_1^2} \tag{24}$$

Let us take a look at experimental determination of the dissipative parameter ε. Fixing a value of θ, e.g. $\theta = 2$, consider absolute values of the complex amplitude S_ϑ for some values of parameter ε. Results of calculations for $\nu = 0.5$ are shown in Figure 4. As it is shown above, for large enough values of a results for other values of Poisson's ratio should be similar to those given in Figure 4. Suppose that parameters z_0, G_0, ρ and the horizontal force amplitue Q_0 are known. We can find the value of ω corresponding to the taken value of $\theta = 2$, and carry out an experiment to determine the amplitude $|\hat{u}_\vartheta|$ for a value of r leading to the corresponding value of a according to Equation (15b). After determination of the associated values of $|S_\vartheta|$, we can use the curves shown in Figure 4 to estimate the dissipative parameter ε.

It is important to have results concerning normalized amplitudes of vibration $|S_\vartheta|$ for a wide range of basic parameters a, θ, ε. The envelope curves for maximum of amplitudes based on calculations for a large number of values of parameter θ are shown in Figure 5 for $\nu = 0.5$. These

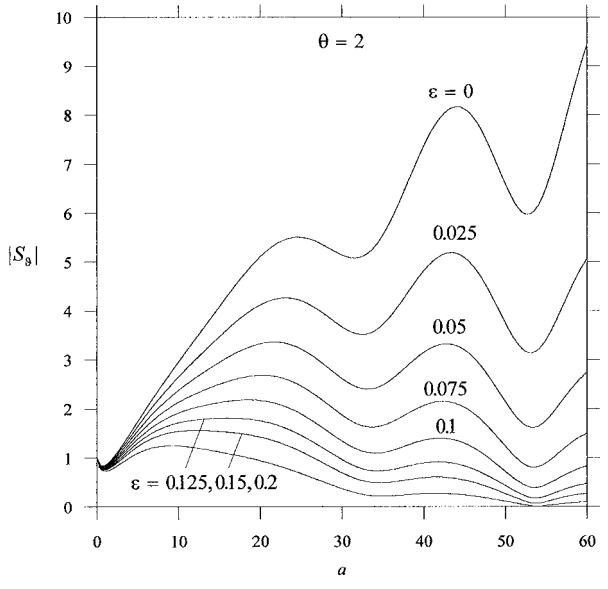

Figure 4. Absolute values of normalized horizontal amplitudes for the fixed value of parameter $\theta = 2$ and several values of parameter ε.

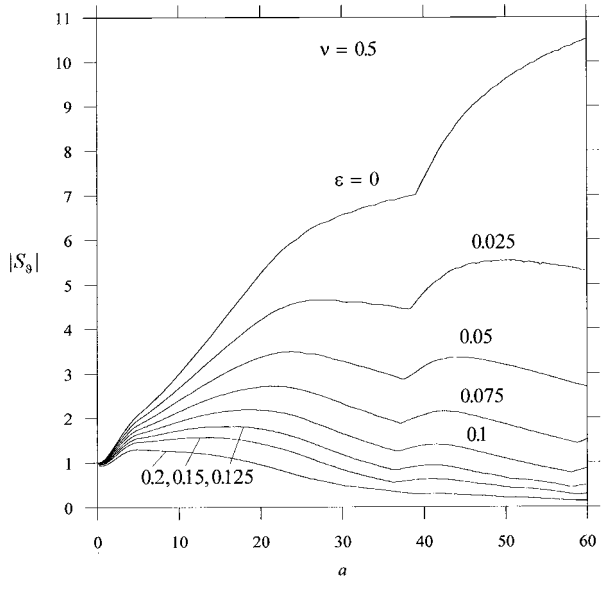

Figure 5. Envelope curves for normalized horizontal amplitudes for different values of dissipative parameter ε.

results can be used also for other values of Poisson's ratio. An important conclusion from this illustration is that inhomogeneity can lead to significant growth of the normalized amplitudes of vibration, which does not take place for a homogeneous half-space in the considered case of horizontal vibrations. This growth is explained by the existence of Love's waves in an inhomogeneous half-space.

CASE B: A VERTICAL FORCE

The vertical amplitudes at the surface of the half-space in the case of a point vertical force will be studied with the help of the following expression [12]:

$$u_z = \frac{P_0(1-\nu)}{2G_0\pi r} S_{vv} \tag{25}$$

where the factor before S_{vv} is the static value for the corresponding homogeneous half-space. First we considered the phase angle δ_V of complex normalized amplitudes S_{vv}. In the present case, the corresponding curves are less close to straight lines than in the case of the amplitudes u_ϑ. As an example, in Figure 6(a), several curves are shown for non-dissipative case ($\varepsilon = 0$) and the value of Poisson ratio $\nu = 1/3$. We see that the phase angle changes abruptly for values of θ close to 0.47. This is explained by the fact that the absolute values of the complex amplitude passes practically through zero for $\theta \approx 0.47$, $a \approx 39$ [see Figure 6(b) which shows a number of curves for θ close to 0.47]). Similar behaviour is observed also for other values of parameters ε, ν, θ. We will consider the second and third waves as in the case of the amplitudes u_ϑ and draw the secant line through the points corresponding to the phase angles -2π, -4π (second wave) and -4π, -6π (third wave). Analogous to Equation (16) we write the equation for the secant lines in the form

$$\delta_V = b_V - k_V a \tag{26}$$

where b_V a constant which does not influence wavelengths and k_V is the non-dimensional wave number [similar to k_ϑ in relationship (16)]. In Figure 7, the dependence k_V on parameter λ defined by Equation (18) is shown for $\varepsilon = 0$ and 0.1 and $\nu = 1/3$. Discontinuities are for those values of θ for which amplitude can be close to zero on the corresponding interval. Unlike the case of horizontal vibrations studied above, more noticeable difference between the results for the second and third waves takes place. For applying the obtained theoretical results to experimental determination of properties of soil, we will consider large enough values of θ ($\theta > 0.8$–1) to avoid discontinuities.

Let us take a look at determination of the equivalent depth, i.e the depth to which we can relate properties of soil corresponding to characteristics of surface waves. Using the dimensional wave number K_V which is related to the non-dimensional wave number k_V analogous to relationship (17b) phase velocity C for considered vertical displacements can be written in the form

$$C = \frac{\omega}{K_V} = \frac{\omega}{k_V \omega \sqrt{\rho/G_0}} = \frac{1}{k_V}\sqrt{\frac{G_0}{\rho}} \tag{27}$$

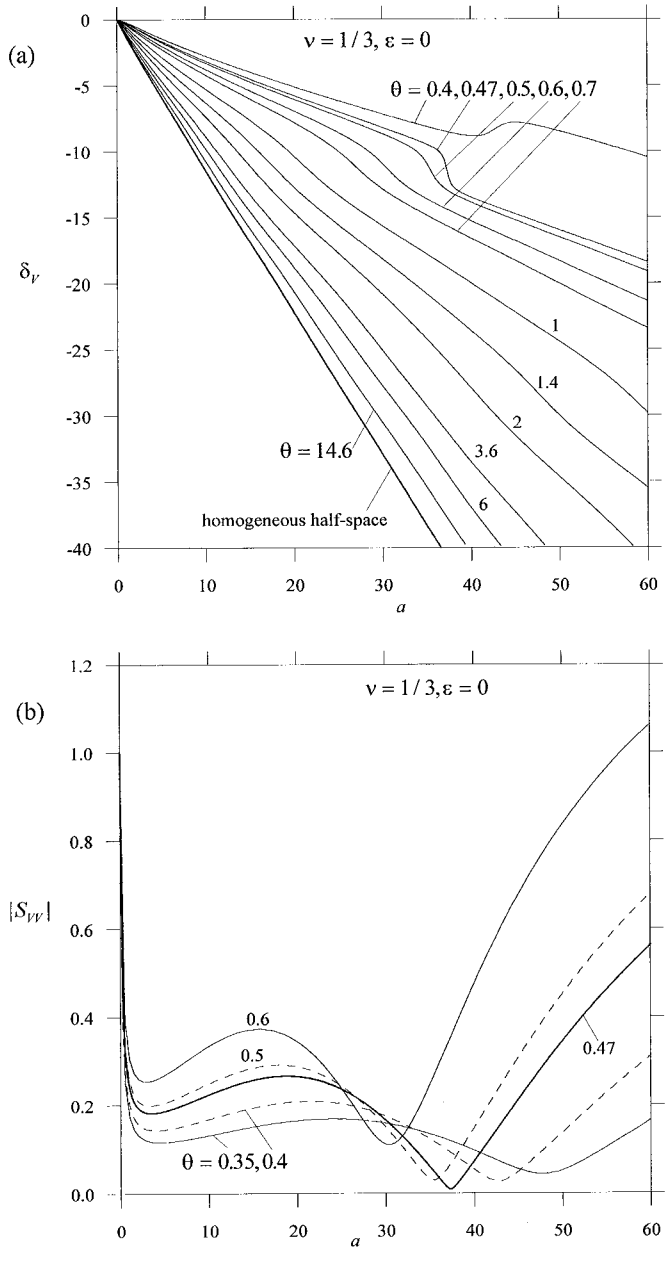

Figure 6. Phase angle (a) of complex vertical amplitudes of vibrations and absolute values (b) of normalized vertical amplitudes for the values of θ leading to an abrupt variation of the phase angle.

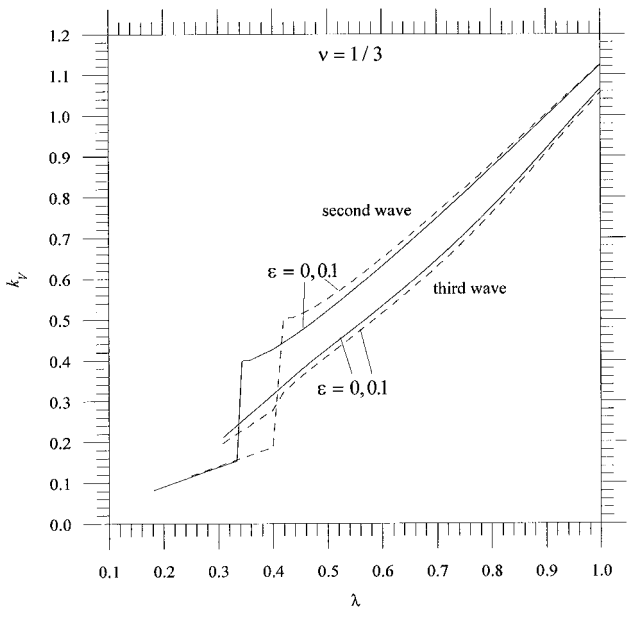

Figure 7. Non-dimensional wave number k_V versus parameter λ for vertical vibrations.

Introduce the shear modulus G_h corresponding to the value C provided a half-space is homogeneous

$$G_h = k_{Vh}^2 C^2 \rho = \frac{k_{Vh}^2}{k_V^2} G_0 \tag{28}$$

where k_{Vh} is non-dimensional wave number for homogeneous half-space which is taken for the same wave (second or third) as k_V. Note that for $\nu = 1/3$, $\varepsilon = 0$ computations give $k_{Vh} = 1.1238$ and $k_{Vh} = 1.0660$ for the second and third waves, respectively (the value of k_{Vh} for pure Rayleigh waves is 1.0724). According to Equation (28) the relation G_h/G_0 (or k_{Vh}^2/k_V^2) is a function of parameter θ, which can be expressed through the non-dimensional wavelength $\tilde{l}$ (see Equation (23a)):

$$\tilde{l} = \frac{l}{z_0} = \frac{2\pi}{k_V(\theta)\theta} \tag{29}$$

The dependence for the value G_h/G_0 on $\tilde{l}$ is shown in Figure 8 for the second and third waves. These graphs allow a good approximation with the help of the function

$$\frac{G_h}{G_0} \approx (1 + \gamma \tilde{l}\,)^{\zeta} \tag{30}$$

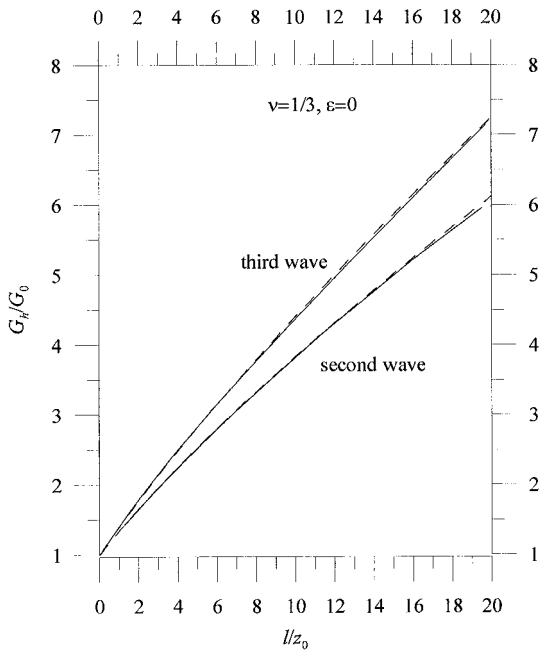

Figure 8. Ratio G_h/G_0 versus non-dimensional wavelength.

where $\gamma = 0.46$, $\zeta = 0.78$ for the second wave and $\gamma = 0.51$, $\zeta = 0.82$ for the third wave. The dashed lines in Figure 8 represent the function (30). Note that the interval of $\tilde{l}$-variation represented in Figure 8 corresponds to the interval for $\theta : 0.8 < \theta < \infty$ for which discontinuities for wave number are absent. In order to obtain relation between the equivalent depth H and wavelength l equate the value G_h/G_0 (as the function of $\tilde{l}$) to the shear modulus divided by G_0 at depth H. Equation (11) leads to

$$\frac{G_h}{G_0} = 1 + \tilde{H} \tag{31}$$

where $\tilde{H} = H/z_0$. Finally, we find

$$\frac{H}{l} = \left(\frac{G_h}{G_0} - 1\right) \Big/ \tilde{l} \tag{32}$$

According to Equation (32) the ratio H/l is determined by inclinations of secant lines for curves shown in Figure 8. Figure 9 shows that H/l as a function of the non-dimensional wavelength $\tilde{l}$ for $\nu = 1/3$ and $\varepsilon = 0$; dashed lines corresponds to the approximate relation (30). A noticeable deviation between results for the second and third waves is observed. We see that the ratio H/l decreases with the wavelength growth and this fact has to be taken into account when interpreting experimental data.

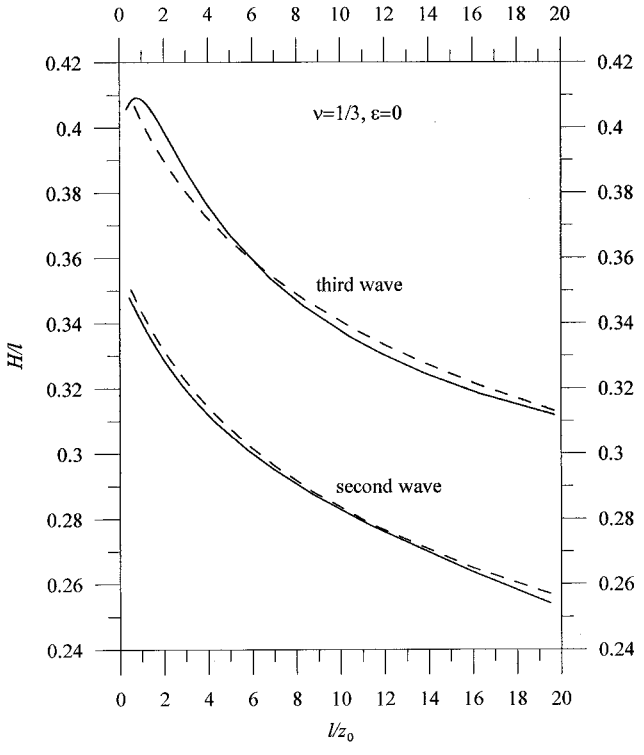

Figure 9. Ratio of equivalent depth to wavelength versus non-dimensional wavelength.

Now consider how one can define soil properties using measurements of the wavelengths l at definite frequencies for surface vertical amplitudes due to a vertical harmonic force. Assume we know values C_1, l_1 and C_2, l_2 for two values of frequencies f_1 and f_2. Using Equation (28) and (30) we can write

$$\frac{C_2^2}{C_1^2} = \frac{(1 + \gamma(l_2/z_0))^\zeta}{(1 + \gamma(l_1/z_0))^\zeta} \tag{33}$$

$$z_0 = \gamma \frac{C_2^{2/\zeta} l_1 - C_1^{2/\zeta} l_2}{C_1^{2/\zeta} - C_2^{2/\zeta}} \tag{34}$$

Knowing z_0 and l_1 the value G_h/G corresponding to l_1 can be found from Figure 8 or with the help of relationship (30). Thereafter the related value of k_V is determined according to equation (28):

$$k_V^2 = \frac{k_{Vh}^2}{G_h/G_0} \tag{35}$$

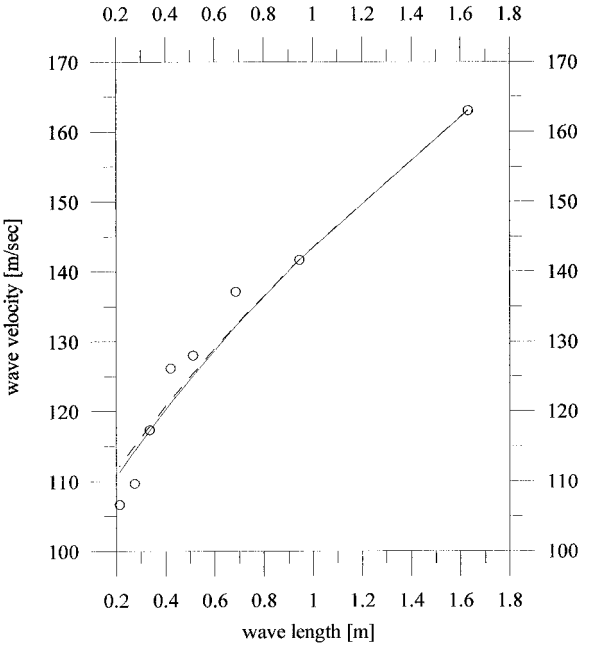

Figure 10. Comparison of experimental results from Reference [16] (circles) and theoretical results for second (dashed line) and third (solid line) waves.

and we can find the shear modulus G_0 from Equation (27) (assuming the density ρ is known):

$$G_0 = C_1^2 k_V^2 \rho \tag{36}$$

As one example, consider the data given in Reference [16, p. 114] relating to a silty fine sand. Here, for some values of frequencies, the corresponding average wavelengths and velocities are given. We use these values assuming that they are related to second or third waves and taking $\nu = 1/3$, $\varepsilon = 0$. Let us take the following values from Reference [16]: $f_1 = 100$ Hz, $l_1 = 1.631$ m (5.35 ft), $C_1 = 163.1$ m/s (535 ft/s) and $f_2 = 150$ Hz, $l_2 = 0.945$ m (3.1 ft), $C_1 = 141.7$ m/s (465 ft/s). Equation (34) leads to $z_0 = 0.294$ m for the second wave and $z_0 = 0.376$ m for the third wave. According to Equation (30) for $l = l_1$ the value G_h/G_0 is equal 2.685 and 2.604 for the second and third waves, respectively. For $\rho = 1800\,\mathrm{kg/m^3}$ with the help of equations (35) and (36) we obtain for the second and third waves: $G_0 = 22.51$ and $20.89\,\mathrm{MN/m^2}$. Based on the latter results we can find for given values of wavelengths corresponding theoretical values of G_h/G_0 and afterwards wave velocities C from Equation (28). Comparison of the experimental (from Reference [16]) and theoretical values of C is given in Figure 10, where circles represent experimental data, dashed (solid) line is for theoretical results corresponding to the second (third) wave. Although parameters z_0 and G_0 are noticeably different for the second and third waves (which leads to two significantly different half-spaces) the result concerning wave velocities are very close to each other. The model of linearly inhomogeneous half-space seems to be very good for the approximating of the considered experimental data.

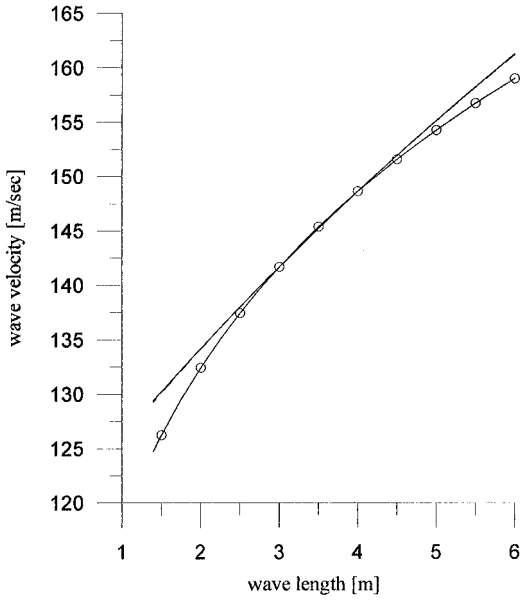

Figure 11. Comparison of results based on an experiment from Reference [18] (line with circles) and theoretical results for second (dashed line) and third (solid line) waves.

As one more example, consider the data given in Reference [18] where a relation (based on experimental data) between the surface wave velocity C and the wavelength l is presented for a sandy gravel in the form

$$C = 118l^{1/6} \tag{37}$$

where l is given in m and C in m/s. Experiments were carried out for frequencies significantly lower than in the first example, the interval of wavelengths is $1.4\,\text{m} < l < 6.2\,\text{m}$. Using the above presented procedure for $l_1 = 4\,\text{m}$, $l_2 = 3\,\text{m}$ and the corresponding values of C_1 and C_2 according to Equation (37) we find (taking $v = 1/3$, $\rho = 1800\,\text{kg/m}^3$) for the second wave: $z_0 = 2.14\,\text{m}$, $G_0 = 30.95\,\text{MN/m}^2$ and for the third wave: $z_0 = 2.58\,\text{m}$, $G_0 = 28.04\,\text{MN/m}^2$. In Figure 11, wave velocities are represented versus wavelengths for relationship (37) (line with circles), for the second wave (dashed line) and the third wave (solid line).

Let us look at the influence of dissipative parameter ε on the surface amplitudes of vertical vibrations due to a vertical force. In Figure 12, absolute values of normalized amplitudes S_{VV} are presented for $\theta = 3.2$ and values of Poisson ratio $v = 1/3$. These curve can be used for the determination of the damping parameter ε as in the case of horizontal vibration considered above. Envelope curves for amplitudes of vibration are presented in Figure 13 for $v = 1/3$; these curves allow us to estimate maximum values of amplitudes for a very wide range of all parameters entering the considered problem.

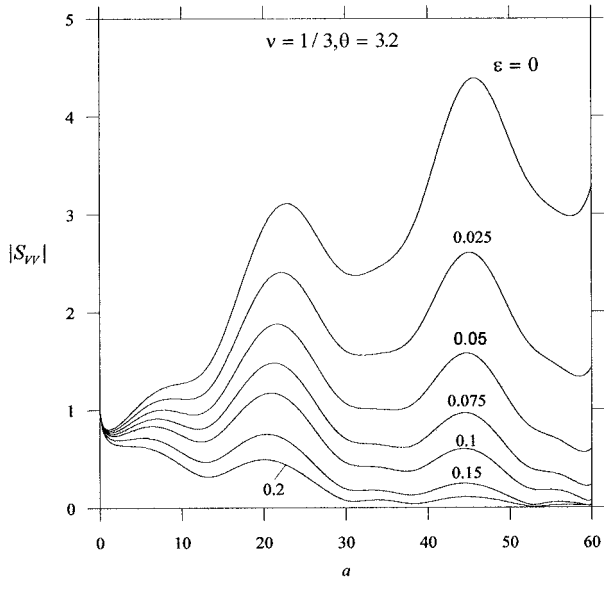

Figure 12. Absolute values of normalized vertical amplitudes of vertical vibrations for the fixed value of parameter θ and different values of dissipative parameter ε.

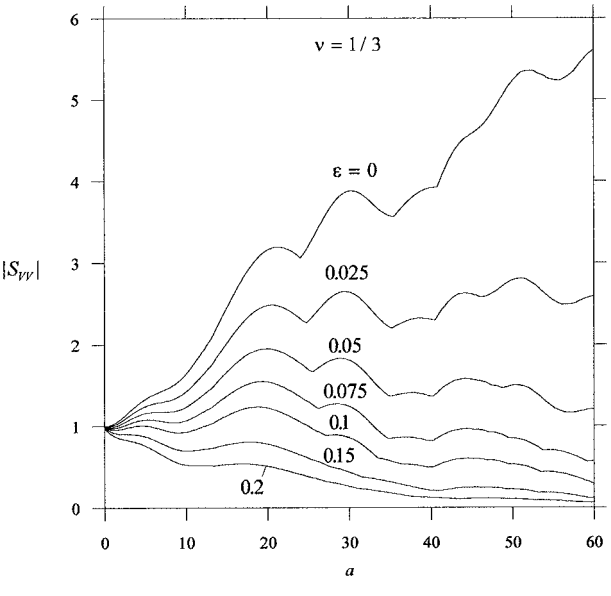

Figure 13. Envelope curves for normalized vertical amplitudes for different values of dissipative parameter ε.

CONCLUSION

In this paper, the horizontal vibration of points at the surface of a linearly inhomogeneous elastic half-space excited by a surface time-harmonic horizontal force and vertical vibration due to a vertical force are studied in detail in order to build up a basis for experimental determination of properties of soil foundations: degree of inhomogeneity realized by parameter z_0 in the considered linear variation of the shear modulus, the shear modulus at the surface of the half-space, G_0, and dissipative parameter ε. Calculations show a definite relation between the parameter, θ, which takes into account the degree of inhomogeneity and frequency of vibration, and the slope of phase angle curves of complex amplitudes of vibration. These curves can noticeably differ from a straight line. For this reason secant lines for the phase angle curves are introduced which correspond to different numbers of waves: 'second wave' for the phase interval $(-2\pi, -4\pi)$, 'third wave' for the interval $(-4\pi, -6\pi)$, and so on; analysis of slopes of the secant lines leads to desired relations between parameters of the linearly inhomogeneous half-space and wave characteristics. Results for the horizontal force allow a simple approximation for the relationship between parameter λ (associated with θ) and non-dimensional wave number; based on experimental data, this gives an easy way for determination of parameters of the considered theoretical model. Also in the case of vertical vibrations generated by a vertical force results of calculations are represented in a form that allows an effective determination for the required parameters of the considered model. The study of the so-called equivalent depth shows that its ratio to a wavelength decreases with the wavelength growth. For the vertical vibration in the case of low frequencies, points on the surfaces of the linearly inhomogeneous half-space with amplitudes of vibration close to zero exist; this phenomenon is a result of an interference of different waves propagating through the inhomogeneous half-space. These points lead to discontinuities in phase angle curves which makes application of the considered wave propagation technique difficult in the case of low frequencies ($\theta < 0.8$–1) or long wavelengths ($l/z_0 > 20 - 25$).

REFERENCES

1. Awojobi AO. Vertical vibration of a rigid circular foundation on Gibson soil. *Geotechnique* 1972; **22**: 333–343.
2. Awojobi AO. Vibration of rigid bodies on non-homogeneous elastic semi infinite elastic media. *Quarterly Journal of Mechanics and Applied Mathematics* 1973; **26**:483–498.
3. Rao CRA, Goda MAA. Generalization of Lamb's problem to a class of inhomogeneous elastic half-spaces, *Proceedings of the Royal Society of London* 1978; **A359**: 93–110.
4. Vrettos Ch. In-plane vibration of soil deposits with variable shear modulus: II. Line load. *International Journal for Numerical and Analytical Methods in Geomechanics* 1990; **14**:649–662.
5. Vrettos Ch. Forced anti-plane vibrations at the surface of an inhomogeneous half-space. *Soil Dynamics and Earthquake Engineering* 1991; **10**:230–235.
6. Vrettos Ch. Time-harmonic Boussinesq problem for a continuously non-homogeneous soil. *Earthquake Engineering & Structural Dynamics*. 1991; **20**:961–977.
7. Gazetas G. Static and dynamic displacements of foundations on heterogeneous multilayered soils. *Geotechnique* 1980; **30**:159–177.
8. Muravskii G, Operstein V. Time-harmonic vibration of an incompressible linearly non-homogeneous half-space. *Earthquake Engineering & Structural Dynamics* 1996; **25**:1195–1209.
9. Muravskii G. Green functions for an incompressible linearly inhomogeneous half-space. *Archieves of Applied Mechanics* 1996; **67**:81–95.
10. Muravskii G. Time-harmonic problem for a non-homogeneous half-space with exponentially varying shear modulus. *International Journal of Solids and Structures* 1997; **34**:3119–3139.
11. Muravskii G. On time-harmonic problem for non-homogeneous elastic half-space with shear modulus limited at infinite depth. *European Journal of Mechanics A /Solids* 1997; **16**:227–294.

12. Muravskii G. Green functions for a compressible linearly inhomogeneous half-space. *Archieves of Applied Mechanics* 1997; **67**:521–534.
13. Stoneley R. The transmission of Rayleigh waves in a heterogeneous medium. *Geophysical Supplement to the Monthly Notices of the Royal Astronomical Society*, London 1934; **3**:222–232.
14. Vardoulakis I, Vrettos C. Dispersion-law of Rayleigh-type waves in a compressible Gibson half-space, *International Journal for Numerical and Analytical Methods in Geomechanics* 1988; **12**:639–655.
15. Vardoulakis I. Surface waves in a half-space of submerged sand. *Earthquake Engineering & Structural Dynamics* 1981; **9**:329–342.
16. Richart Jr. FE, Hall Jr. JR, Woods RD. *Vibrations of Soils and Foundations*. Prentice-Hall; Englewood Cliffs, NJ, 1970.
17. Vrettos Ch. In-plane vibration of soil deposits with variable shear modulus: I. *Surface waves. International Journal for Numerical and Analytical Methods in Geomechanics* 1990; **14**:209–222.
18. Vrettos Ch, Prange B. Evaluation of *in situ* effective modulus from dispersion measurements. *Journal of Geotechnical Engineering* 1990; **116**:1581–1585.
19. Nazarian S, Stokoe KH. In situ shear wave velocities from spectral analysis of surface waves. *Proceedings of the Eighth World Conference on Earthquake Engineering*, vol. 3, 1984; 31–38.
20. Stokoe KH, Nazarian S. Use of Rayleigh waves in liquefaction studies. In *Measurements and Use of Shear Wave Velocity*, Woods RD (ed.), ASCE 1985; 1–17.
21. Gucunski N, Woods RD. Inversion of Rayleigh wave dispersion curve for SASW test, *Proceedings of the* 1*st International Conference on Soil Dynamics and Earthquake Engineering*, Karlsruhe, 1991; 127–138.
22. Gucunski N, Woods RD. Numerical simulation of the SASW test, *Soil Dynamics and Earthquake Engineering* 1992; **11**:213–227.
23. Rix GJ, Leipski EA. Accuracy and resolution of surface wave inversion. *Conference on Recent Advances in Insturmentation Data Acquisition and Testing in Soil Dynamics* 1991; 17–32.
24. Gazetas G. Vibrational characteristics of soil deposits with variable wave velocity. *International Journal for Numerical and Analytical Methods in Geomechanics* 1982; **6:**1–20.
25. Thomson WT. Transmission of elastic waves through a stratified soil medium. *Journal of Applied Physics* 1950; **21**:89–93.
26. Haskell NA. The dispersion of surface waves in multilayered media. *Bulletin of the Seismological Society of America* 1953; **43**:17–34.
27. Leung KL, Vardoulakis IG, Beskos DE, Tassoulas JL. Vibration isolation by trenches in continuously non-homogeneous soil by the BEM. *Soil Dynamics and Earthquake Engineering* 1991; **10**:172–179.
28. Kausel E, Roesset JM. Stiffness matrices for layered soils. *Bulletin of the Seismological Society of America* 1981; **71**:1743–1761.

